High thermal stability of correlated color temperature using current compensation in hybrid warm white high-voltage LEDs

Kuo-Ju Chen,[1] Hsuan-Ting Kuo,[1] Hsin-Chu Chen,[1] Min-Hsiung Shih,[1,2*]
Chao-Hsun Wang,[1] Shih-Hsuan Chien,[1] Sheng Huan Chiu,[1] Chien-Chung Lin,[3]
Ching-Jen Pan,[4] and Hao-Chung Kuo[1,4]

[1] *Department of Photonics & Institute of Electro-Optical Engineering, National Chiao Tung University, Hsinchu 30010, Taiwan*
[2] *Research Center for Applied Sciences, Academia Sinica, Taipei 11529, Taiwan*
[3] *Institute of Photonic System, National Chiao Tung University, Tainan 711, Taiwan*
[4] *hckuo@faculty.nctu.edu.tw*
[5] *Helio Photonics Cooperation, Taiwan*
[*] *mhshih@gate.sinica.edu.tw*

Abstract: This study experimentally and numerically examines the correlated color temperature (CCT) stability issue for hybrid warm white high-voltage light-emitting diodes (HV-LEDs) by using a current compensation method. This method could efficiently maintain the CCT stability factor at approximately 1.0 and yield greater color uniformity with $\Delta u'v'$ values ranging from 0.017 to 0.003 in CIE 1976 chromaticity coordinates. The simulation results show that the red chip intensity drop is the primary cause of CCT instability in the hybrid warm white system when the temperature increases. Therefore, Furthermore, results indicate that the relative lumen drop improves from 21% to 15% by using a current compensation method.

References and links

1. E. F. Schubert and J. K. Kim, "Solid-state light sources getting smart," Science **308**(5726), 1274–1278 (2005).
2. S. Nakamura, T. Mukai, and M. Senoh, "Candela-class high-brightness INGAN/ALGAN double-heterostructure blue-light-emitting diodes," Appl. Phys. Lett. **64**(13), 1687–1689 (1994).
3. H. S. Jang and D. Y. Jeon, "Yellow-emitting Sr_3SiO_5: Ce^{3+},Li^+ phosphor for white-light-emitting diodes and yellow-light-emitting diodes," Appl. Phys. Lett. **90**(4), 041906 (2007).
4. S. Pimputkar, J. S. Speck, S. P. DenBaars, and S. Nakamura, "Prospects for LED lighting," Nat. Photonics **3**(4), 180–181 (2009).
5. Y. S. Tang, S. F. Hu, W. C. Ke, C. C. Lin, N. C. Bagkar, and R. S. Liu, "Near-ultraviolet excitable orange-yellow $Sr_3(Al_2O_5)Cl_2$: Eu^{2+} phosphor for potential application in light-emitting diodes," Appl. Phys. Lett. **93**(13), 131114 (2008).
6. H. C. Chen, K. J. Chen, C. H. Wang, C. C. Lin, C. C. Yeh, H. H. Tsai, M. H. Shih, H. C. Kuo, and T. C. Lu, "A novel randomly textured phosphor structure for highly efficient white light-emitting diodes," Nanoscale Res. Lett. **7**(1), 188 (2012).
7. W. Im, N. N. Fellows, S. P. DenBaars, and R. Seshadri, "$La_{1-x-0.025}Ce_{0.025}Sr_{2+x}Al_{1-x}Si_xO_5$ solid solutions as tunable yellow phosphors for solid state white lighting," J. Mater. Chem. **19**(9), 1325–1330 (2009).
8. W. Im, N. George, J. Kurzman, S. Brinkley, A. Mikhailovsky, J. Hu, B. F. Chmelka, S. P. DenBaars, and R. Seshadri, "Efficient and Color-Tunable Oxyfluoride Solid Solution Phosphors for Solid-State White Lighting," Adv. Mater. (Deerfield Beach Fla.) **23**(20), 2300–2305 (2011).
9. Y. Zhang, L. Wu, M. Ji, B. Wang, Y. Kong, and J. Xu, "Structure and photoluminescence properties of $KSr_4(BO_3)_3$:Eu^{3+} red-emitting phosphor," Opt. Mater. Express **2**(1), 92–102 (2012).
10. H. Li, H. K. Yang, B. K. Moon, B. C. Choi, J. H. Jeong, K. Jang, H. S. Lee, and S. S. Yi, "Tunable photoluminescence properties of Eu(II)- and Sm(III)-coactivated $Ca_9Y(PO_4)_7$ and energy transfer between Eu(II) and Sm(III)," Opt. Mater. Express **2**(4), 443–451 (2012).
11. S. K. K. Shaat, H. C. Swart, and O. M. Ntwaeaborwa, "Synthesis and characterization of white light emitting $Ca_xSr_{1-x}Al_2O_4$:Tb^{3+},Eu^{3+} phosphor for solid state lighting," Opt. Mater. Express **2**(7), 962–968 (2012).

12. R. M. Farrell, E. C. Young, F. Wu, S. P. DenBaars, and J. S. Speck, "Materials and growth issues for high-performance nonpolar and semipolar light-emitting devices," Semicond. Sci. Technol. **27**(2), 024001 (2012).
13. H. Zhao, G. Liu, J. Zhang, J. D. Poplawsky, V. Dierolf, and N. Tansu, "Approaches for high internal quantum efficiency green InGaN light-emitting diodes with large overlap quantum wells," Opt. Express **19**(S4), A991–A1007 (2011).
14. H. Zhao and N. Tansu, "Optical gain characteristics of staggered InGaN quantum wells lasers," J. Appl. Phys. **107**(11), 113110 (2010).
15. J. Zhang and N. Tansu, "Improvement in spontaneous emission rates for InGaN quantum wells on ternary InGaN substrate for light-emitting diodes," J. Appl. Phys. **110**(11), 113110 (2011).
16. S. H. Park, D. Ahn, J. Park, and Y. T. Lee, "Optical Properties of Staggered InGaN/InGaN/GaN Quantum-Well Structures with Ga- and N-Faces," Jpn. J. Appl. Phys. **50**(7), 072101 (2011).
17. Y. K. Ee, J. M. Biser, W. Cao, H. M. Chan, R. P. Vinci, and N. Tansu, "Metalorganic Vapor Phase Epitaxy of III-Nitride Light-Emitting Diodes on Nanopatterned AGOG Sapphire Substrate by Abbreviated Growth Mode," IEEE J. Sel. Top. Quantum Electron. **15**(4), 1066–1072 (2009).
18. Y. Li, S. You, M. Zhu, L. Zhao, W. Hou, T. Detchprohm, Y. Taniguchi, N. Tamura, S. Tanaka, and C. Wetzel, "Defect-reduced green GaInN/GaN light-emitting diode on nanopatterned sapphire," Appl. Phys. Lett. **98**(15), 151102 (2011).
19. Y. J. Lee, C. H. Chiu, C. C. Ke, P. C. Lin, T. C. Lu, H. C. Kuo, and S. C. Wang, "Study of the Excitation Power Dependent Internal Quantum Efficiency in InGaN/GaN LEDs Grown on Patterned Sapphire Substrate," IEEE J. Sel. Top. Quantum Electron. **15**(4), 1137–1143 (2009).
20. E. Rangel, E. Matioli, Y. S. Choi, C. Weisbuch, J. S. Speck, and E. L. Hu, "Directionality control through selective excitation of low-order guided modes in thin-film InGaN photonic crystal light-emitting diodes," Appl. Phys. Lett. **98**(8), 081104 (2011).
21. X. H. Li, R. Song, Y.-K. Ee, P. Kumnorkaew, J. F. Gilchrist, and N. Tansu, "Light Extraction Efficiency and Radiation Patterns of III-Nitride Light-Emitting Diodes with Colloidal Microlens Arrays With Various Aspect Ratios," IEEE Photonics J. **3**(3), 489–499 (2011).
22. D. S. Meyaard, G. B. Lin, Q. Shan, J. Cho, E. F. Schubert, H. Shim, M. H. Kim, and C. Sone, "Asymmetry of carrier transport leading to efficiency droop in GaInN based light-emitting diodes," Appl. Phys. Lett. **99**(25), 251115 (2011).
23. H. Zhao, G. Liu, R. A. Arif, and N. Tansu, "Current injection efficiency induced efficiency-droop in InGaN quantum well light-emitting diodes," Solid-State Electron. **54**(10), 1119–1124 (2010).
24. C. H. Wang, S. P. Chang, P. H. Ku, J. C. Li, Y. P. Lan, C. C. Lin, H. C. Yang, H. C. Kuo, T. C. Lu, S. C. Wang, and C. Y. Chang, "Hole transport improvement in InGaN/GaN light-emitting diodes by graded-composition multiple quantum barriers," Appl. Phys. Lett. **99**(17), 171106 (2011).
25. C. Sommer, F. P. Wenzl, P. Hartmann, P. Pachler, M. Schweighart, S. Tasch, and G. Leising, "Tailoring of the color conversion elements in phosphor-converted high-power LEDs by optical simulations," IEEE Photon. Technol. Lett. **20**(9), 739–741 (2008).
26. Y. Shuai, Y. He, N. T. Tran, and F. G. Shi, "Angular CCT Uniformity of Phosphor Converted White LEDs: Effects of Phosphor Materials and Packaging Structures," IEEE Photon. Technol. Lett. **23**(3), 137–139 (2011).
27. C. Sommer, P. Hartmann, P. Pachler, M. Schweighart, S. Tasch, G. Leising, and F. P. Wenzl, "A detailed study on the requirements for angular homogeneity of phosphor converted high power white LED light sources," Opt. Mater. **31**(6), 837–848 (2009).
28. Z. Liu, S. Liu, K. Wang, and X. Luo, "Optical Analysis of Color Distribution in White LEDs With Various Packaging Methods," IEEE Photon. Technol. Lett. **20**(24), 2027–2029 (2008).
29. H. C. Kuo, C. W. Hung, H. C. Chen, K. J. Chen, C. H. Wang, C. W. Sher, C. C. Yeh, C. C. Lin, C. H. Chen, and Y. J. Cheng, "Patterned structure of remote phosphor for phosphor-converted white LEDs," Opt. Express **19**(S4), A930–A936 (2011).
30. C. H. Wang, D. W. Lin, C. Y. Lee, M. A. Tsai, G. L. Chen, H. T. Kuo, W. H. Hsu, H. C. Kuo, T. C. Lu, S. C. Wang, and G. C. Chi, "Efficiency and Droop Improvement in GaN-Based High-Voltage Light-Emitting Diodes," IEEE Electron Device Lett. **32**(8), 1098–1100 (2011).
31. Y. H. Won, H. S. Jang, K. W. Cho, Y. S. Song, D. Y. Jeon, and H. K. Kwon, "Effect of phosphor geometry on the luminous efficiency of high-power white light-emitting diodes with excellent color rendering property," Opt. Lett. **34**(1), 1–3 (2009).
32. S. E. Brinkley, N. Pfaff, K. A. Denault, Z. Zhang, H. T. Hintzen, R. Seshadri, S. Nakamura, and S. P. DenBaars, "Robust thermal performance of $Sr_2Si_5N_8$:Eu^{2+}: An efficient red emitting phosphor for light emitting diode based white lighting," Appl. Phys. Lett. **99**(24), 241106 (2011).
33. H. K. Lee, D. H. Lee, Y. M. Song, Y. T. Lee, and J. S. Yu, "Thermal measurements and analysis of AlGaInP/GaInP MQW red LEDs with different chip sizes and substrate thicknesses," Solid-State Electron. **56**(1), 79–84 (2011).
34. D. P. Bour, D. W. Treat, R. L. Thornton, R. S. Geels, and D. F. Welch, "Drift leakage current in AlGAInP quantum-well lasers," IEEE J. Quantum Electron. **29**(5), 1337–1343 (1993).
35. N. T. Tran and F. G. Shi, "Studies of Phosphor Concentration and Thickness for Phosphor-Based White Light-Emitting-Diodes," J. Lightwave Technol. **26**(21), 3556–3559 (2008).

1. Introduction

Light-emitting diodes (LEDs) have been regarded as the next generation of environment lighting sources because of its long lifetime, high efficiency, and energy-saving properties, especially in solid-state lighting (SSL) [1–4]. Using blue chips with yellow phosphor has recently become the most common method for generating white light sources [5,6]. Therefore, great efforts have been made to synthesize the novel phosphor with III-Nitride LEDs in the recent years [7–11]. As for the part in the InGaN-based LEDs chips, the progress in white LEDs is strongly driven by the advances in high efficiency InGaN-based LEDs emitting in the visible spectral regime [12–24]. These InGaN-based LEDs are used as high-power pump excitation sources in phosphor-based white LEDs. Recent works by using new types of active regions with reduced charge separation [12–16], growths and substrate technologies [17–19], nano/microphotonics structures [20,21], and barrier engineering [22–24] have led to significant improvement in nitride-based LEDs. Thus, the availability of high efficiency nitride LEDs enables the practical implementation of phosphor-based white LEDs. As a replacement for traditional lamps, high lumen efficacy and suitable color quality are critical standards for white LEDs. The quality of white LEDs is determined by correlated color temperature (CCT) homogeneity and high color rending index (CRI), which can be further improved [25]. Several studies have focused on reducing CCT deviation [26,27]. Liu et al. proposed that the phosphor location influences CCT performance [28]. Furthermore, the patterned remote phosphor structure has also been shown to obtain high chromatic stability [29]. Therefore, the control of CCT deviation in white LEDs has become the critical issue to replace the conventional incandescent light for SSL applications.

Conversely, recent research on high-voltage light-emitting diodes (HV-LEDs) has indicated that multiple series-connected micro-diodes in a single large chip obtains high forward voltage with a low driving current, thereby reducing current crowding and efficiency droop [30]. Additionally, two types of color temperature primarily exist for SSL: cool white and warm white. Red phosphor is frequently adopted in phosphor composition to achieve lower color temperatures at approximately 3000 K as a warm white lighting source and a higher CRI [31,32]. Furthermore, it has recently been proposed that the hybrid warm white HV-LED systems comprising blue chips, phosphor, and red chips achieve greater luminous efficacy and CRI values compared with previous warm white technology. However, the AlGaInP material used in red LEDs is sensitive to temperature variation, thereby resulting in a significant intensity drop compared with other systems [33]. Moreover, the dominant drift leakage in AlGaInP is also important to emphasize at the high temperature [34]. Therefore, varying thermally intensity drops and wavelength shift behavior between blue and red chips potentially causes CCT instability at different temperatures.

In this study, the characteristics of hybrid warm white HV-LEDs investigated experimentally and numerically. This is the first time the current compensation method has been proposed to obtain uniformity of angular CCT in hybrid white warm HV-LEDs. CCT deviation maintains similar values from 20 to 90 °C using the current compensation method. Furthermore, the lumen drop behavior is improved slightly with the increased temperature. Consequently, the color deviation $\Delta u'v'$ value is characterized with CIE 1976 chromaticity coordinates.

2. Experiments and simulation

The hybrid warm white system is composed of four 45 x 45 mil InGaN blue HV-LEDs, two 50 x 25 mil AlGaInP red HV-LEDs, and yellow phosphor powder (YAG:Ce, approximately 15 μm). The domain peak emission wavelength of our blue LEDs and red LEDs are 452 and 617 nm, respectively. The electric circuit for InGaN HV-LEDs and AlGaInP HV-LEDs are independent in the system to demonstrate the current compensation method. For comparison, a constant 20 mA input current on both blue and red chips is used for in the conventional

system, whereas the proposed system is treated using the current compensation method with a constant 20 mA current for blue chips and a tunable current (15 to 25 mA) for red chips to control red light intensity and maintain CCT stability. Moreover, the luminous efficiency of HV-LEDs is 100 lm/W, and the CRI is 90 at approximately 3000 K, with a 20 mA driving current. Figure 1 shows the temperature dependence of the HV-LED emission spectra. The peak shift and intensity drop transform especially the red chip. Furthermore, the parameters for peak shift and intensity drop as a function of increased temperature are shown in Table 1. However, these phenomena cause a significant deviation in CCT and consequent instability in white LEDs.
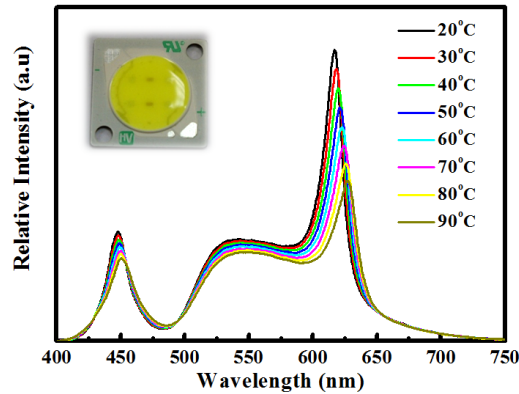

Fig. 1. Temperature-dependent emission spectra of the hybrid warm white HV-LEDs. The inset shows the sample for the hybrid warm white HV-LEDs.

Table 1. Peak wavelength and intensity drop at each temperature

Ta(°C)	20	30	40	50	60	70	80	90
Wp(nm)	617	618	620	621	623	624	626	627
Drop(%)	0	7	13	20	27	33	39	46

This study employs the OptisWorks simulation software based on the Monte-Carlo method to analyze the influence of the thermally dependent intensity drop and wavelength shift of red chips on CCT of the hybrid warm white system [29]. In the simulation, the parameters of the refractive index in phosphor, silicone, and the air are set to 1.82, 1.54, and 1.0, respectively. The dimensions of the chips are fixed at 45 x 45 mil for the InGaN blue HV-LED and 50 x 25 mil for the AlGaInP red HV-LED. As for the phosphor layer, the particle sizes and the concentration of phosphor are set as average diameter of 12 μm and 8%, which is uniform distributed in the silicon binder. Moreover, the shape of the phosphor layer is designed as the slightly convex and the thickness of the phosphor layer is about 300 μm in the middle. The phosphor absorbs the blue light from the LED chips and emits the isotropic yellow light and the amount of light being absorbed and scattered by phosphor particles are simulated using Mie Theory [35]. The reflectance of the surface on the board and reflector is about 90% in the simulation. The additional procedures are as follows: First, the simulated structure included two red chips and four blue chips in the phosphor mixture, and then the measured spectra at different temperatures were input into the simulation model. Thereafter, the thermal dependent wavelength shift and intensity drop are two calculated values in the simulation. For the wavelength shift, the peak wavelength of the red chip is shifted from 617 to 627 nm (the same as our experimental results in Table 1), as shown in Fig. 2(a). The CCT in the simulation result shows a similar value and indicates that the spectrum shift of the red ship is not the primary reason for CCT instability, as shown in the inset of Fig. 2(a). For the peak wavelength, the red chip spectrum at various light output intensities from 100% to 46% with identical peak wavelengths is entered into the simulation software (Fig. 2(b)). CCT

increases at approximately 1000 K with a 47% intensity drop. Therefore, the instability of CCT in hybrid white warm HV-LEDs may be attributable to the red chip intensity drop, rather than the spectrum shift, and become critical when the ambient temperature increases.
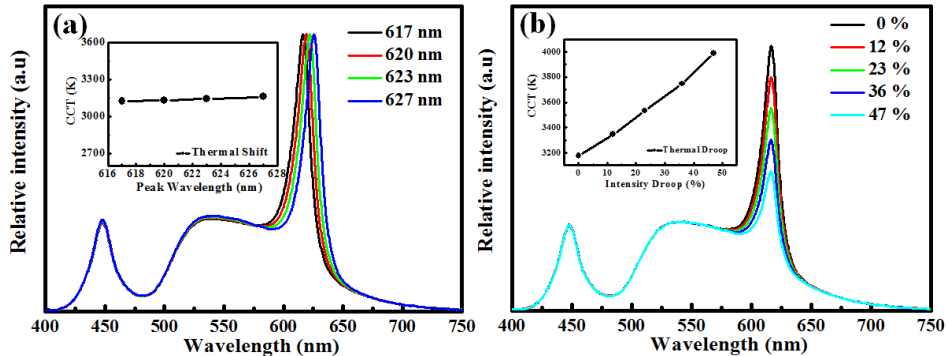

Fig. 2. (a) The simulation spectra with different peak wavelengths of red chip. The inset shows the simulation results on CCT with different peak wavelength of red chip (b) The simulation spectrums with different red chip intensity. The inset shows the simulation result on CCT with different red chip intensity.

From the simulation results, the red chip intensity drop in the hybrid warm white LEDs is the primary cause of CCT instability. The wavelength shifts of the LED chips are the minor factors in CCT instability. Thus, the concept of using the current compensation method to increase the red chip intensity is proposed, especially at high ambient temperatures. In this experiment, an integrated sphere is employed for optical characteristics measurement, a thermoelectric cooler for thermal control, and two power sources for applying different currents to the red chip and blue chip separately. The current compensation method in HV-LEDs is shown with a constant 20 mA input current for blue chips and a tunable current for the red chips at a room temperature of 90 °C. To maintain the sample CCT, the input current of the red chip is increased with the ambient temperature. Therefore, CCT stability can be obtained at various temperatures. Additionally, this experiment is designed to simulate a real case in hybrid warm white systems and solve CCT instability.

4. Results and discussion

The warm white light source is used for indoor lighting, and its CCT stability is crucial. Therefore, the CCT stability factor is defined as the variations in CCT value at different temperatures divided by the CCT at the initial temperature. The CCT stability factor with and without current compensation at various ambient temperatures is shown in Fig. 3. The CCT deviation in hybrid warm white HV-LED with current compensation is improved and maintains a similar value at different temperatures, compared with the device without current compensation. Furthermore, the CCT stability factor maintains a value greater than 0.99, regardless of the temperature using current compensation method, whereas the factor decreases to 0.88 at the ambient temperature of 90 °C in the reference. This result indicates that the red chip intensity drop is the primary factor influencing CCT variation. This finding is consistent with the simulation results. In addition, the compensated current for the red chip at various ambient temperatures is shown in Table 2. To obtain a constant CCT, the compensated current increases with the ambient temperature. This advantage in CCT stability is caused by the supplement of higher red light intensity the current compensation. Moreover, the CRI value would be increased due to the stability of the red light with the current compensation method.
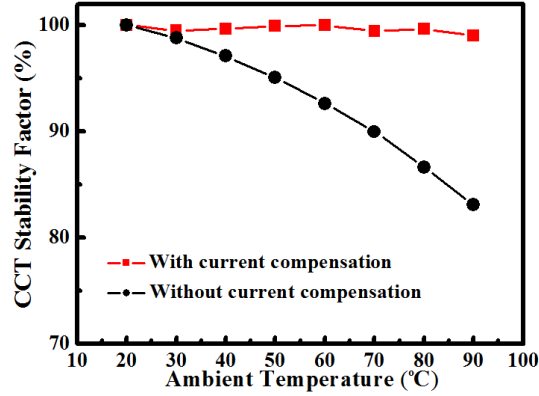
Fig. 3. The CCT Stability Factor of with and without current compensation at different ambient temperature

Table 2. The compensated current in red chip at different ambient temperatures

Ta(°C)	20	30	40	50	60	70	80	90
Compensated Current (mA)	16	17	18	19	20	21	23	25

The normalized lumen efficacy and luminous efficiency of the two samples with and without current compensation, as a function of ambient temperature, were investigated (Fig. 4(a) and 4(b)). The lumen drop is improved from 21% to 15% by using current compensation. With the increase in ambient temperature, the differences of lumen drop between the two samples become greater. This indicates that the heat generation inside the LEDs increases, thereby reducing lumen efficacy. However, the results show that the current compensation method in hybrid white warm HV-LEDs maintains an identical flux output, confirming the practicality of this method for SSL applications. As for the luminous efficiency, the hybrid warm white LED with current compensation is higher than the conventional one due to the less electrical power from 20°C to 50°C. It obtains the same luminous efficiency at 60°C because of the same electrical power in red chip. With the increase temperature after 70 °C, the luminous efficiency of hybrid warm white LED with current compensation is lower than the conventional one because of the higher driven current in the red LED chips.
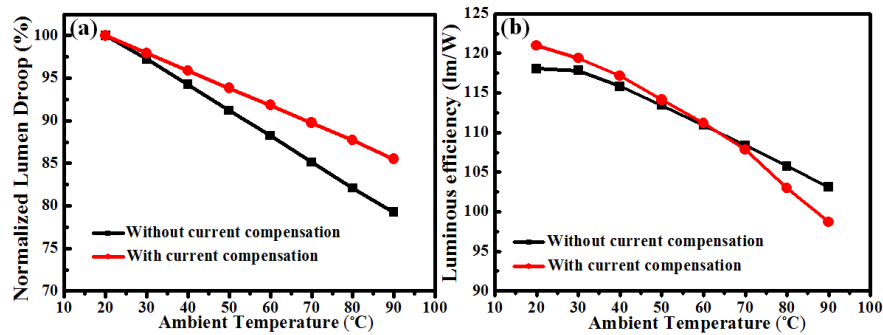

Fig. 4. (a) The relative lumen drop (b) luminous efficiency with and without current compensation at different ambient temperature

To compare the color distribution between two samples, the color deviation of a lighting system, ($\Delta u'v'$) is calculated as follows:

$$u' = 4x/(-2x+12y+3) \tag{1}$$

$$v' = 9y / (-2x + 12y + 3) \qquad (2)$$

$$\Delta u'v' = \sqrt{(\Delta u')^2 + (\Delta v')^2} \qquad (3)$$

where u', v' is the chromaticity coordinates in the CIE 1976 diagram, and x and y are the chromaticity coordinates in the CIE 1931 diagram, as shown in Eqs. (1) and (2). The $\Delta u'v'$ value indicates spatial color uniformity in Eq. (3). Figure 5 shows the color chromaticity coordinate deviations at various ambient temperatures from 20 to 90 °C. The chromaticity coordinates in both samples move to the blue region as the temperature increases. The experimental $\Delta u'v'$ value shows that the hybrid white warm HV-LEDs using current compensation yields a significantly greater color uniformity than that of the reference when the temperature increases from 20 to 90 °C (Fig. 5(a)). Furthermore, the maximum $\Delta u'v'$ value is 0.003 and the reference is 0.017, indicating CCT stability when using current compensation. Consequently, the current compensation method results in significant CCT stability and high-quality SSL.
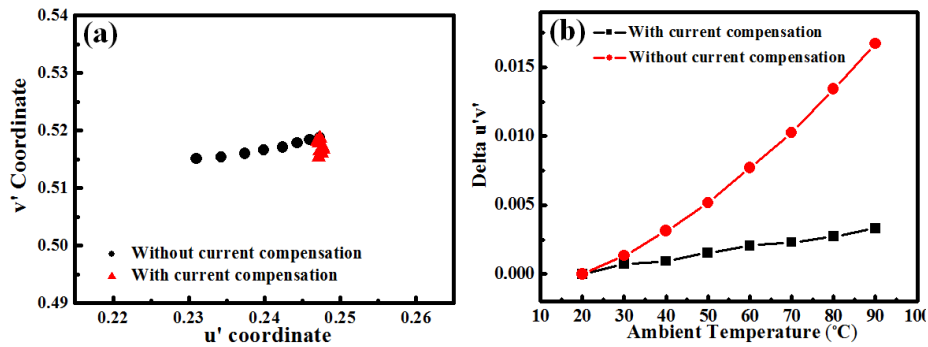

Fig. 5. (a) CIE 1976 chromaticity indices versus various ambient temperatures with and without current compensation (b) Delta $\Delta u'v'$ of the two samples at various ambient temperatures.

4. Conclusion

The current compensation method is employed on a hybrid warm white HV-LEDs system comprising blue chips, phosphor, and red chips. The simulation results show that the red chip intensity drop influences CCT instability more than the peak wavelength shift. Furthermore, the CCT stability factor is calculated to estimate the light quality in LEDs, and a similar value is maintained using the current compensation method. Thus, the greater color uniformity with $\Delta u'v'$ values from 0.017 to 0.003 in CIE 1976 chromaticity coordinates. Furthermore, the relative lumen drop and CCT stability are improved using this method. This method is anticipated to be a suitable candidate for use in warm white HV-LEDs for SL applications.

Acknowledgment